Materials Science-Poland, 39(4), 2021, pp. 599-614
http://www.materialsscience.pwr.wroc.pl/
DOI: 10.2478/msp-2021-0046

Al_2O_3-TiO_2 coatings deposition by intermixed and double injection SPS concepts

Monika Nowakowska[1,*], Paweł Sokołowski[1], Tomáš Tesař[2], Radek Mušálek[2], Tomasz Kiełczawa[1]

[1]Wroclaw University of Science and Technology, Wrocław, Poland
[2]Institute of Plasma Physics of the Czech Academy of Science, Prague, Czech Republic

This work focuses on the study on the novel hybrid method of simultaneous spraying from two different materials (Al_2O_3 and TiO_2) by means of suspension plasma spraying (SPS) using submicron powder and water suspension. The goal was to attempt the deposition of intermixed alumina-titania coatings, namely: Al_2O_3 + 3 wt.% TiO_2, Al_2O_3 + 13 wt.% TiO_2, and Al_2O_3 + 40 wt.% TiO_2. Such compositions are already used but in the form of conventionally plasma sprayed coatings, with micrometer-sized powder. Meanwhile, the injection of feedstocks with submicron-sized particles has not been established yet. In particular, this paper uses two routes of feedstock injection, (i) with the use of an intermixed suspension and (ii) a double injection of separate suspensions. The attention was paid to the characterization of the feedstock materials, description of deposition parameters as well as the morphology, microstructure, and phase composition of the obtained coatings. Among all coatings, Al_2O_3 + 40 wt.% TiO_2 sprayed with double injection contained the most homogeneously distributed and melted splats. The results from this work demonstrate the possibility of coating deposition both by intermixed and double injection concepts but also the need for the further application-relevant optimization, related to the presence of intercolumnar gaps in the microstructure of the coatings.

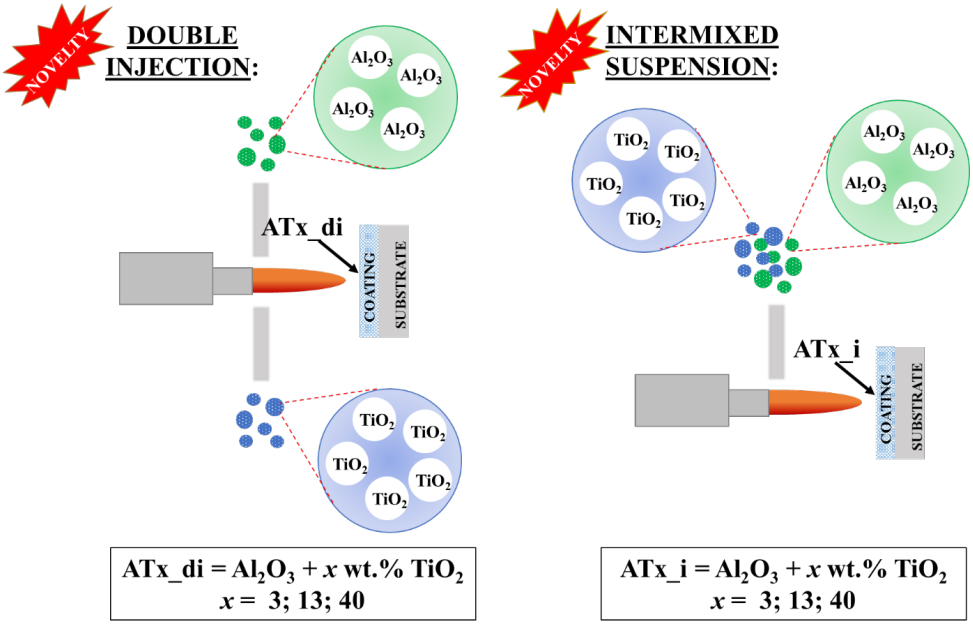

Keywords: *suspension plasma spraying, alumina-titania coatings, intermixed suspension, double injection, microstructure*

* E-mail: monika.m.nowakowska@pwr.edu.pl

1. Introduction

Suspensions, introduced several years ago as a novel, liquid type of feedstock material [1], opened up new opportunities for thermal spraying, including suspension plasma spraying (SPS), suspension-based high velocity oxy-fuel spraying (S-HVOF) and others [2]. Replacement of the coarse, dry, powder with the particle sizes on the order of tens to hundreds of micrometers by the fine powder-based suspension allowed the obtaining of submicrometer or even nanometer-sized features in the coatings [3] or even entirely new microstructures, such as the columnar-like coatings [4]. The particular advantage of using suspension feedstocks is the possibility to tailor the coating microstructure to the specific application – for example, dense coatings for heater tubes for hydraulic parts [5] or extremely porous coatings for filtration purposes [6]. On the other hand, it should be emphasized that liquid feedstock spraying processes are far more complex than the powder-based ones. The challenges that have emerged are: formulation of a stable suspension, proper feedstock injection and uniform fragmentation of the suspension in the jet, extensive substrate heating due to a shorter spray distance, and many others [7].

This paper covers the study on the coatings of the Al_2O_3-TiO_2 system, which is considered as one of the most useful and versatile material/coating arrangements. Al_2O_3 coatings are widely used for replacement parts in turbines and bearings or biomedical implants due to their high hardness, elastic modulus, favorable adhesion, and anti-wear properties [8]. However, their tribological and fracture toughness properties are not on a par with other ceramic coatings, such as Cr_2O_3 [9], TiO_2 [5], ZrO_2 [9], YSZ [10], etc. [11]. From a technical perspective, this limits their use in applications where the simultaneous improvement in hardness, elastic modulus, and fracture toughness is required [12]. To tackle the issue, many research groups incorporated various materials into the Al_2O_3 matrix. One of them is TiO_2, due to its beneficial influence on fracture toughness. Alumina-titania coatings were sprayed mainly by the conventional plasma spraying method [13], with the use of micrometer-sized powders [14]. Only several trials were carried out to deposit these coatings from suspensions, to study the effect of particle size [15], phase composition [16], and wear properties [9], including also our previous studies published in [17] and [18]. Coatings studied in this paper will be regarded for the contents of TiO_2 equal to 3, 13, and 40 wt.% (AT3, AT13, AT40), which are typical compositions sprayed by the conventional powder spraying [19]. However, the idea of obtaining composite Al_2O_3/TiO_2 coatings can be more easily realized by liquid feedstock thermal spraying by virtue of their much finer splats/structural features allowing a more intensive mixing of the components. Composite suspension plasma sprayed coatings were already investigated also for other material combinations, for example: Al–Si/B_4C [20], Cr_2O_3–TiO_2 [21] or 8YSZ with graphene oxide (GO) [22].

Such multi-material coatings can be obtained in different ways, i.e., by: (i) incorporation of agglomerated or sintered powders, where one powder particle has a complex chemical composition [23], (ii) simultaneous deposition of two separate feedstocks [24], (iii) spraying of layered microstructures [25], (iv) building of a gradient structure, where one material passes gradually into another one, and (v) incorporation of fine nano platelets, which are employed as the reinforcement of monolithic coating [11]. Currently, the main approach is the so-called hybrid spraying. However, the term ‘hybrid’ is used in different contexts. In most cases, the idea involves simultaneous feeding of two various feedstocks [4], like (i) a suspension with nano- or submicron powder particles [26] and (ii) a powder of micrometer size [27]. Coatings obtained by two different types of feedstocks showed promising results in enhancing the functional performance [28] but most of the authors recommend further process optimization to increase deposition efficiency, improve coatings functional properties [27] and process applicability [29]. An alternative possibility to the proposed method is the injection of two various liquid feedstocks via two separate feeding lines, e.g., two suspensions [4]. This route may be favored in comparison to the former one, due to the similar and small size of all powder particles. As a result, a higher contact area between the vari-

Table 1. Characteristic of suspensions used for the Al_2O_3-TiO_2 coatings deposition

Coating code	Target composition	Used suspensions		Solvent
AT3_i	Al_2O_3 + 3 wt.% TiO_2	intermixed Al_2O_3 and TiO_2, to have Al_2O_3 + 3 wt.% TiO_2		H_2O
AT3_di	Al_2O_3 + 3 wt.% TiO_2	Al_2O_3	TiO_2	H_2O
AT13_i	Al_2O_3 + 13 wt.% TiO_2	intermixed Al_2O_3 and TiO_2, to have Al_2O_3 + 13 wt.% TiO_2		H_2O
AT13_di	Al_2O_3 + 13 wt.% TiO_2	Al_2O_3	TiO_2	H_2O
AT40_i	Al_2O_3 + 40 wt.% TiO_2	intermixed Al_2O_3 and TiO_2, to have Al_2O_3 + 40 wt.% TiO_2		H_2O
AT40_di	Al_2O_3 + 40 wt.% TiO_2	Al_2O_3	TiO_2	H_2O

i – intermixed suspension, di – double injection

ous materials is possible, leading to homogeneous intermingling of two (or more) different materials [30]. Another concept is spraying of an intermixed suspension, which refers to the deposition of one feedstock via one feeding line (for example: suspension intermixed with fine powder, suspension intermixed with other or solution precursor) [4]. Intermixed constituents travel together in the plasma jet and may be easily melted together. Therefore, they may form small splats, having a high contact area. This, in turn, further favors their mutual interaction, beneficial for the homogeneity of the structure [4]. Nevertheless, the knowledge on hybrid spraying is far from being well established [31].

The proposed study deals with very contemporary subjects in the fields of materials science and surface engineering. On the one hand, the multi-feedstock spraying, where two different materials (namely: Al_2O_3 and TiO_2) are used, is still a novelty in the area of the liquid feedstock deposition. It could bring a synergic effect in the final coating properties (i.e., increased fracture toughness), as well as a tailored microstructure (in the case of alumina-titania coatings, the intended structure should be mainly dense and homogeneous). On the other hand, the comparison of the intermixed and the double injection feedstock delivery provides the details about the spraying feasibility and its influence on the microstructural integrity and phase stability of the coatings.

The aim of the work was to carry out the preliminary study on the hybrid plasma spraying itself and to evaluate the overall microstructure and phase composition of the coatings. By characterizing the mechanism of coating formation, and its basic properties, new, more tailorable, specific coating compositions or microstructures could be considered in the future. These results may also be adapted in other plasma spray technologies that use liquid feedstock, for example Solution Precursor Plasma Spraying (SPPS) or hybrid processes that use both powder and liquid feedstocks.

2. Materials and methods

2.1. Feedstock materials

The study involved the use of two commercially available distilled water-based suspensions: (i) AuerCoat Al_2O_3 25W, Treibacher Industrie, Althofen, Austria, and (ii) AuerCoat TiO_2 25W, Treibacher Industrie, Althofen, Austria. The feedstocks were used in as-produced state for double injection spray experiments. Both suspensions were also used for the formulation of three in-house intermixed feedstocks. They were intended to yield the same target ratio as for the double injection, by means of dilution, namely:

- AT3 (Al_2O_3 + 3 wt.% TiO_2),
- AT13 (Al_2O_3 + 13 wt.% TiO_2),
- AT40 (Al_2O_3 + 40 wt.% TiO_2).

The general scope of study is summarized in the graphical abstract, while the details are provided in Table 1.

2.2. Methods

2.2.1. Feedstock characterization

The studies on feedstock characterization were divided into two stages, including tests on the dried

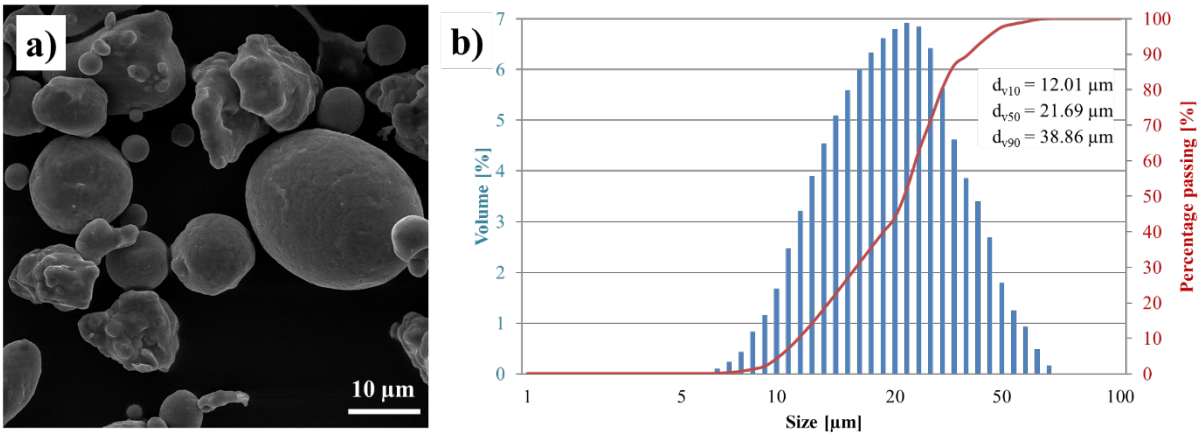

Fig. 1. NiCr bond coat powder: morphology (a) and particle size distribution (b)

Table 2. Deposition parameters of bond coat

Substrate	austenitic stainless steel AISI 304/1.4301, 3 mm thick, diameter 25 mm; sand blasted before spraying (F36 grit, 500–600 µm mesh size) and sonicated with ethanol
Powder	NiCr 80-20, Amdry 4535; dried 3 h before spraying at 110°C
Electric power	27 kW
Injection	radial, external
Stand-off distance	100 mm
Gun	SG-100, Praxair, Indianapolis, USA
Feeding	15 g/min
Transverse velocity	400 mm/s
Plasma gases	Ar/H_2: 45/5 slpm
Carrier gas	Ar 3.5 slpm

powders (morphology, particle size distribution, phase characterization) and the liquid suspension (viscosity, pH, sedimentation tests).

2.2.1.1. Dried powders

The proposed route of using ready-to-spray suspensions was particularly convenient for obtaining coatings without an added time and cost associated with ball milling, stabilization trials, etc. However, these feedstocks need to be subjected to detailed characterization as not all important details are shared by the manufacturers [32]. That is why the suspensions were dried to study the solid phase first.

The powder morphology was examined using a Vega3 SEM microscope (Tescan, Brno, Czech Republic). Powders were gold sputtered before the observation. Then, the powder particle size was verified with a laser diffraction method using a PSA 1190 LD particle size analyzer (Anton Paar, Graz, Austria).

2.2.1.2. Suspensions

The viscosity of the suspensions was measured using a DV2TLV viscometer (Brookfield, USA) with a coaxial cylinder-cylinder geometry. A sequence of speeds from 10 to 100 and back to the 10 RPM with 10 RPM increments (decrements) with taking 5 measurements averaged over 2 s at each speed was set. The values of pH were measured using a HI-2002 Edge pH meter (Hanna Instruments, Leighton Buzzard, UK). The sedimentation test was carried out within 24 hours. Probes with suspensions (diameter 16 mm, liquid level 70 mm) were observed with 10 min intervals within the first hour of testing, and with one hour intervals between the first and the twelfth hour of testing. The last observation was carried out after 24 hours.

Table 3. Deposition parameters and thickness of top coat

	AT3_i	AT3_di	AT13_i	AT13_di	AT40_i	AT40_di
Injection angle, °	25	25	25	25	25	25
Feeding distance, mm	25	25	25	25	25	25
Stand-off distance, mm	100	100	100	100	100	100
Nozzle diameter, mm	0.35	2×0.2	0.35	2×0.2	0.35	2×0.2
Robot speed, mm/s	30	30	30	30	30	30
Carousel speed, RPM	55.5	55.5	55.5	55.5	55.5	55.5
Torch amperage, A	500	500	500	500	500	500
Torch power, kW	150	150	150	150	150	150
Feeding liquid rate, g/min	120	2×37	120	2×37	120	2×37
Feeding pressure, MPa	0.35	0.24	0.35	0.24	0.35	0.24
Interpass substrate temperature, °C	250	250	250	250	250	250
Preheating	yes	yes	yes	yes	yes	yes
Active cooling	air	air	air	air	air	air
Number of deposition cycles	40	140	40	120	40	100
Total number of deposition passes	120	420	120	360	120	300
Net spraying time, min	9.3	32.7	9.3	28	9.3	23.3
Coating thickness, μm	338.2±16.9	241.5±8.2	360.9±16.7	296.7±5.8	316.2±10.9	287.6±8.4
Normalized growth rate, μm/pass	2.82±0.14	1.74±0.06	3.01±0.14	2.24±0.05	2.63±0.09	1.80±0.06

2.2.2. Bond coat deposition

Prior to alumina-titania suspension spraying, the bond coats were deposited first. The deposition of the interlayer was intended mainly to promote the adhesion strength of the top coats. The NiCr 80-20 powder was used, Amdry 4535 (Oerlikon Metco, Wohlen, Switzerland), −53 + 11 μm. The morphology of the bond coat powders is presented in Figure 1a and the particle size of NiCr was also confirmed by laser diffraction. The average size of the powder was equal to d_{v50} = 21.69 μm (Figure 1b).

Bond coats were sprayed by atmospheric plasma spraying using a SG-100 gun (Praxair, Indianapolis, USA). The details of the process are presented in Table 2. The average thickness of the bond coat layer was 61.7±4.8 μm.

2.2.3. Suspension Plasma Spraying

Prior to the spraying, the suspensions were mechanically stirred to redisperse the solid particles. A hybrid water-stabilized plasma torch WSP-H 500 (ProjectSoft HK a.s., Czech Republic) was used for spraying. In total, six coating types were sprayed, namely: AT3_i, AT3_di, AT13_i, AT13_di, A40_i, and AT40_di, where "di" means double injection and "i" – the use of an intermixed suspension. The plasma spray parameters are presented in Table 3. The various feeding rates for intermixed and double injection spray processes relate to different injection systems, and injector diameters, used during spraying. To compare the growth rate for experiments with different solid loads in the feedstocks, growth rate values were normalized for the same solid load feed rate of 30 g/min (like the one used in the experiments: AT3_i, AT13_i, and AT40_i).

The samples were mounted on a rotating carousel, which improved the productivity and repeatability of the deposition (Figure 2).

Prior to the deposition, the samples were preheated by exposition to the plasma jet until they reached 200°C. During the spraying, the samples were continuously actively cooled with compressed air. Additionally, after every 6 deposition

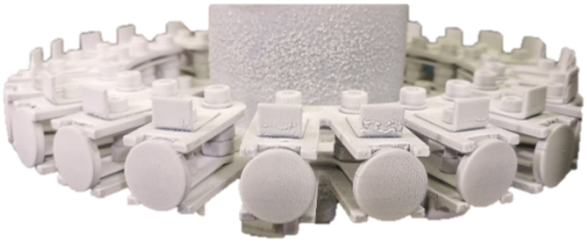

Fig. 2. Carousel with AT3_i coatings after spraying

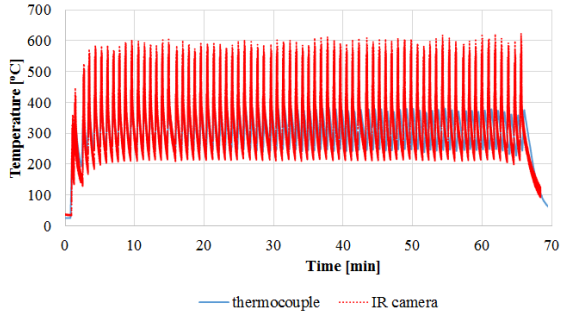

Fig. 3. Temperature of the AT3_di samples recorded with a thermocouple and an IR camera

passes the torch was moved away and the samples were intensively cooled by an air-blade flow. The temperature history was stored both with a thermocamera (coating) and a thermocouple (back side – substrate), see the example in Figure 3.

The feeding pressure was optimized for each suspension by the SprayCam shadowgraphy system (Control Vision Inc, USA), which enabled the observation of droplet fragmentation and trajectory in the plasma jet. Furthermore, the feedstock injection was observed every 15 cycles to confirm the process stability.

2.2.4. Coatings characterization

A microstructural characterization of the surfaces and cross-sections of the top coats (including also the microanalysis by energy-dispersive X-ray, EDX) was carried out with SEM Vega3 (Tescan, Brno, Czech Republic). Due to the poor cohesion of the AT3_di coating (loosely bonded powder particles of micrometer size were easily observed already in a macroscopic state), this sample was excluded from the SEM top view observation. The study on this sample was carried out by a Keyence VHX digital microscope (Keyence, Mechelen, Belgium).

Cross-sections were prepared via standard metallographic preparation, including: cutting of the samples, resin embedding, grinding, polishing, and gold sputtering. The thickness of the top coat was evaluated from at least 5 measurements taken at random locations at a magnification of 500x.

The X-ray diffraction data, both of the feedstock powders and coatings, were obtained using a X'Pert Pro diffractometer with Co Kα radiation. A continuous scan mode with an increment of 0.02° in the scanning range of 10°–110° (2θ) and 0.9 s/step counting time was used.

3. Results and discussion

3.1. Feedstock characterization and the spray process

The raw powders used in commercial alumina and titania suspensions were of similar irregular morphology, built of polyhedral particles (Figure 4).

The powder particle size analysis showed that the particles dried from both suspensions were of a similar size. The Al_2O_3 powders were characterized by d_{v10} = 0.75 µm, d_{v50} = 1.20 µm, and d_{v90} = 2.46 µm, while the TiO_2 feedstock was characterized by d_{v10} = 0.18 µm, d_{v50} = 1.34 µm and d_{v90} = 3.02 µm (Figure 5).

The relationship between the viscosity and the shear rate of the intermixed AT3, AT13, and AT40 suspensions is shown in Figure 6a. Non-Newtonian shear thinning was observed for all feedstocks. According to the study of Tesař et al. [33], who compared stabilized and non-stabilized water-based alumina suspensions, the presence of stabilizing agents increases the suspension's viscosity. However, the information about the chemistry of such agents, their amount, and colloidal details were not specified for the used commercial feedstocks.

Since the sizes of the injector orifice diameter were 0.2 for double injection and 0.35 mm for intermixed, the most important values of the viscosity were at the highest RPMs. This is where the highest shear rate was observed. In this case, all three

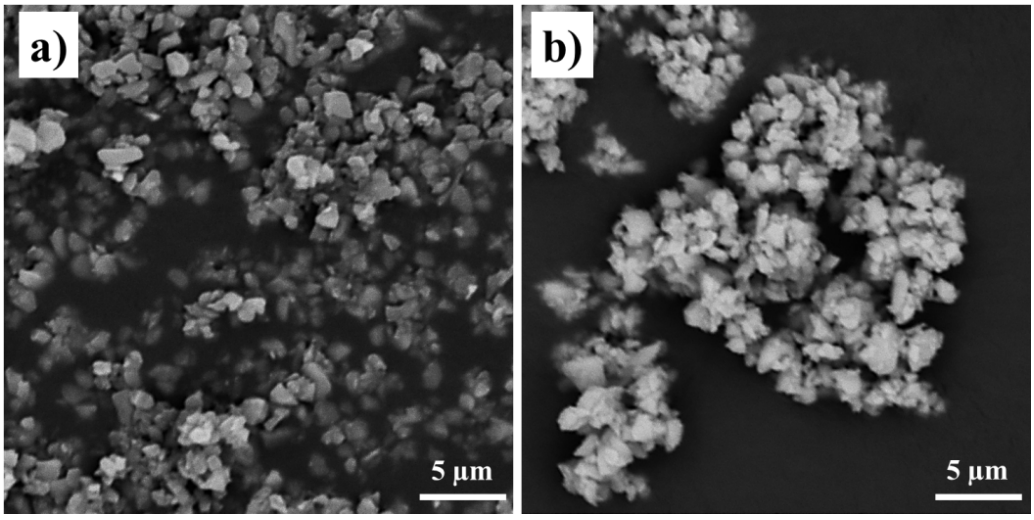

Fig. 4. Morphology of the Al_2O_3 (a) and TiO_2 (b) powders

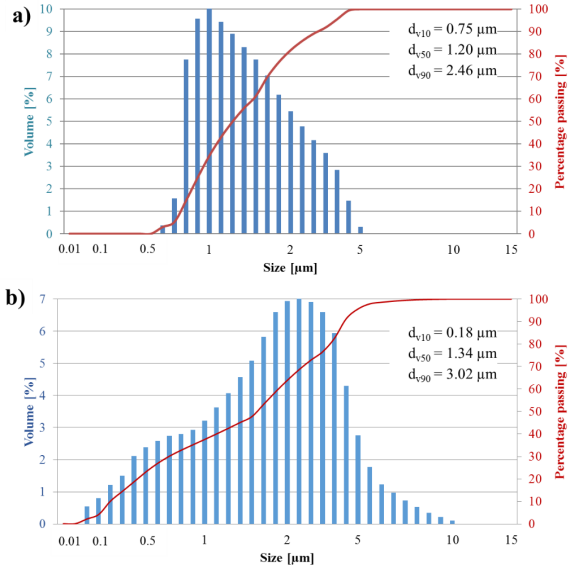

Fig. 5. Particle size distribution of the Al_2O_3 (a) and the TiO_2 (b) powders

suspensions had a similar viscosity. For example, for the shear rate of 100 s^{-1}, the average viscosity values were: η_{AT3} = 7.3 ± 3.2 mPa·s, η_{AT13} = 2.5±0.05 mPa·s, η_{AT40} = 2.0±0.03 mPa·s. This is close to the viscosity of the water solvent: η_{water} = 1.0 mPa·s [33], thus all suspensions were able to be easily fed through the injection nozzles.

Figure 6c and Figure 6d refer to the as-delivered viscosity of the ready-to-spray alumina and titania suspensions. The viscosity of the AuerCoat Al_2O_3 suspension was already studied in the literature but for a solid content of 40 wt.% [33]. Its values ranged from 60 mPa·s at 10 RPM to 20 mPa·s at 100 RPM. In this paper, the alumina suspension contained 25 wt.% of the solid phase and, therefore, the viscosity was lower than presented in work [33]. The obtained values were in the range from 24.3±4.2 mPa·s at 10 RPM to 16.9±2.1 mPa·s at 100 RPM. The behavior of the titania suspension was significantly different from the previous one – the initial viscosity increased, and then reached a lower level. It may be caused by a higher sedimentation speed of the suspensions in comparison to other mixtures, which is discussed later.

The pH value is another important factor when discussing the suspension properties (see Figure 7). It should be between 4 and 10 ideally, to protect the hardware components against corrosion [1]. The measured pH values were within the extreme values of that recommended range. It can be also seen that the values of pH, obtained for the AT3, AT13, and AT40 suspensions, were only slightly lower than the one of Al_2O_3, but the pH value decreased when the rather acidic TiO_2 suspension was added.

Figure 8 presents the levels of the sediment-solvent interfaces observed during the sedimentation tests. Investigations showed that each feed-

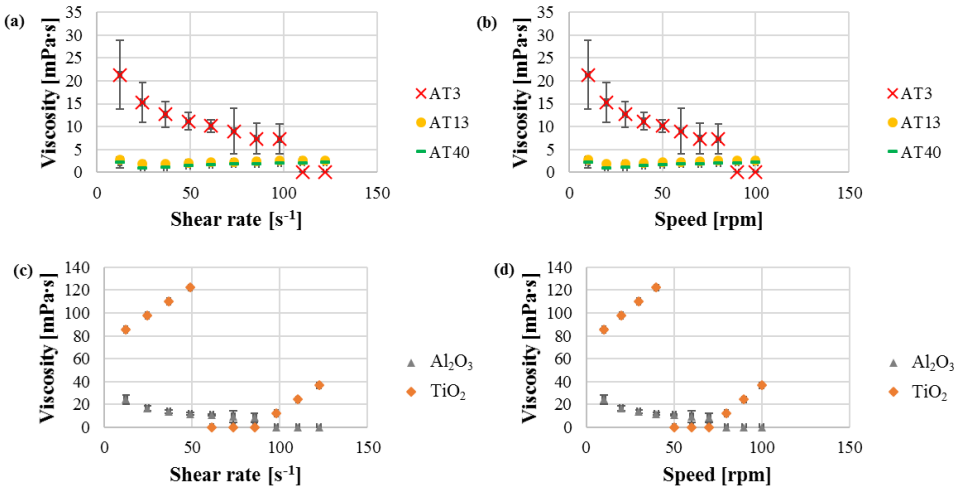

Fig. 6. Relationships between the shear rate and the viscosity of the intermixed (a, b) and the non-intermixed suspensions (c, d)

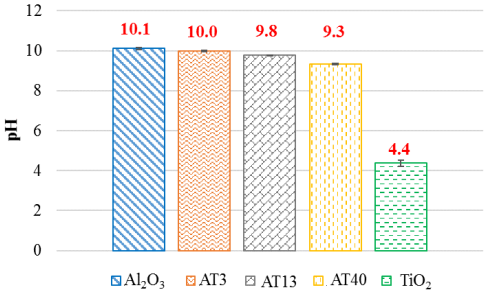

Fig. 7. Values of pH of the studied suspensions

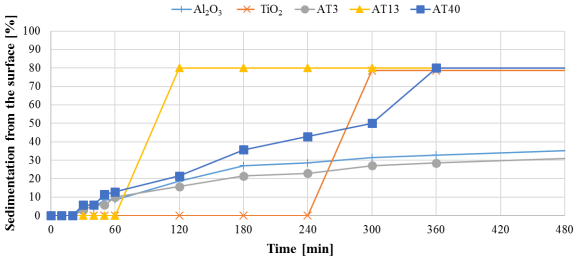

Fig. 8. Sedimentation of the suspensions

stock was stable without any mixing for at least 30 minutes. The TiO_2 and AT13 suspensions displayed a different sedimentation nature than the Al_2O_3, AT3, and AT40 ones. In the first one, the visible sediment-solvent interface was possible to be identified but after 5 hours (TiO_2) and 2 hours (AT13) of testing, the rapid sedimentation was observed in the form of a slurry at the bottom of the probe – the samples reached the saturated state [33]. The most distinguishable interfaces were observed for the AT40 and AT3 suspensions, where a gradual sedimentation was observed. Nevertheless, the spraying of all suspensions was successfully completed by using re-dispersing directly prior to spraying and additional continuous stirring during the deposition process.

Shadowgraphy was used for the visualization of the fragmentation of the liquid droplets in the plasma jet (Figure 9). When comparing the AT3_i, AT13_i, and AT40_i suspensions, it was observed that the behavior of the droplets was similar. Furthermore, in the case of AT3_di, AT13_di, and AT40_di, the liquid droplets penetrated the core of the plasma stream and were quite uniformly fragmented. The injection angle of 25° provided a successful injection of the liquid only in the hot plasma core.

The stability of the spraying was observed during the entire deposition. The double injection was controlled every 15 cycles of the deposition by means of shadowgraphy. As shown in Figure 10 for spray run AT40_di, no disturbances were observed and the fragmentation of the liquid feedstock was similar during the whole spray process.

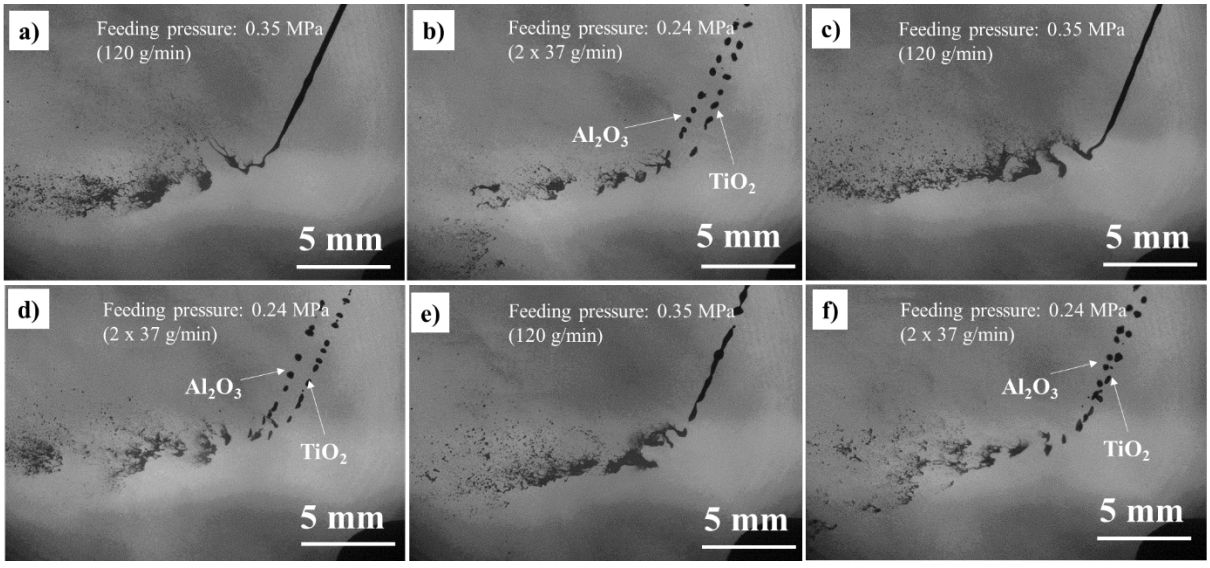

Fig. 9. Fragmentation of the suspension in the plasma jet: AT3_i (a), AT3_di (b), AT13_i (c), AT13_di (d), AT40_i (e), AT40_di (f)

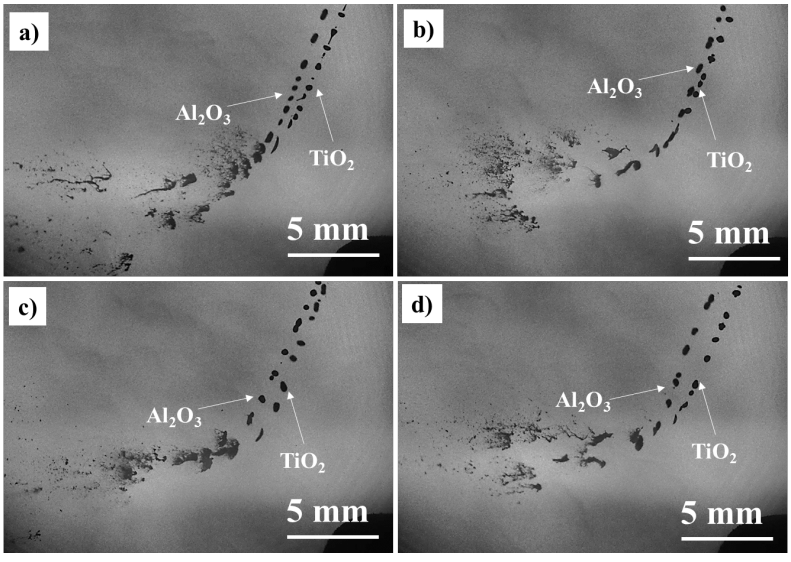

Fig. 10. Fragmentation of the AT40_di suspension in the plasma jet prior 1 spray cycle (a), after 15 cycles (b), after 30 cycles (c), and after 45 cycles (d) of the deposition

3.2. Coatings

The SEM studies on the coating morphology showed that all samples, excluding AT3_di, had a finely-grained, cauliflower-like topography (Figure 11). The AT3_di sample contained a lot of loosely bonded deposits of micrometer size, which was easily observed even during macroscopic observation. However, higher magnification images (see the inserts in Figure 11) revealed that for the other samples (AT3_i, AT13_di, AT40_i), loose particles of submicrometer size remained between the splats. As already reported in the literature [2], this phenomenon is observed for the deposition based on the radial manner of the feedstock injection. During the injection and break-up of the liquid feedstock, some part of it cannot be directly

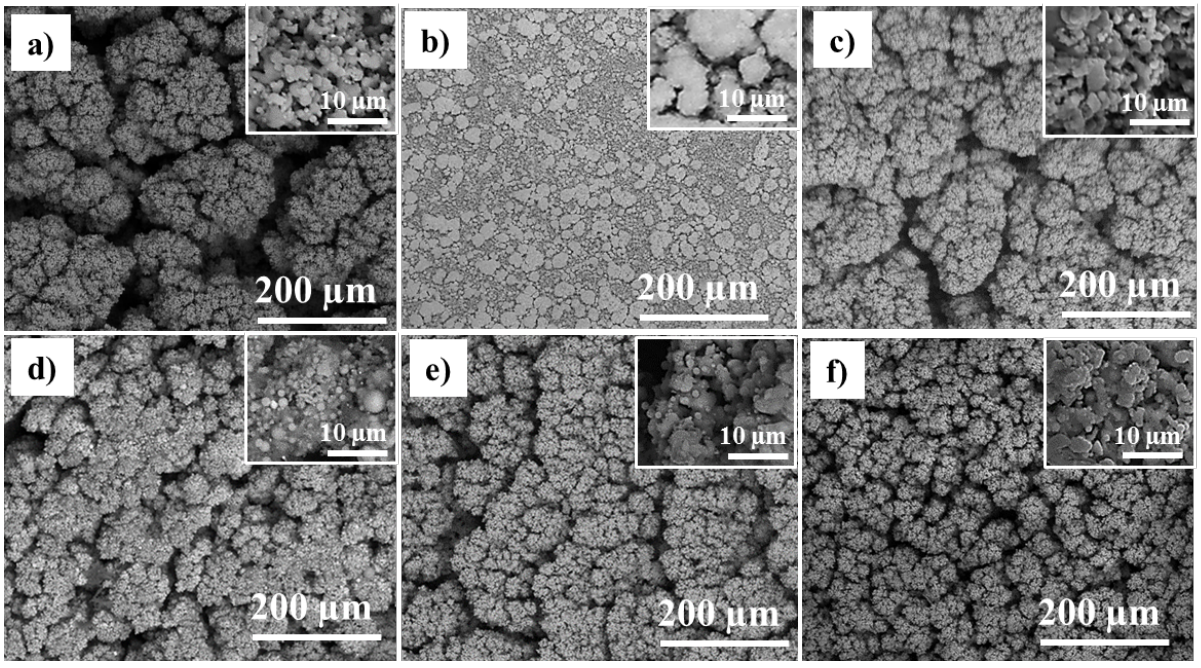

Fig. 11. Topography of the deposited coatings: AT3_i (a), AT3_di (b), AT13_i (c), AT13_di (d), AT40_i (e), AT40_di (f)

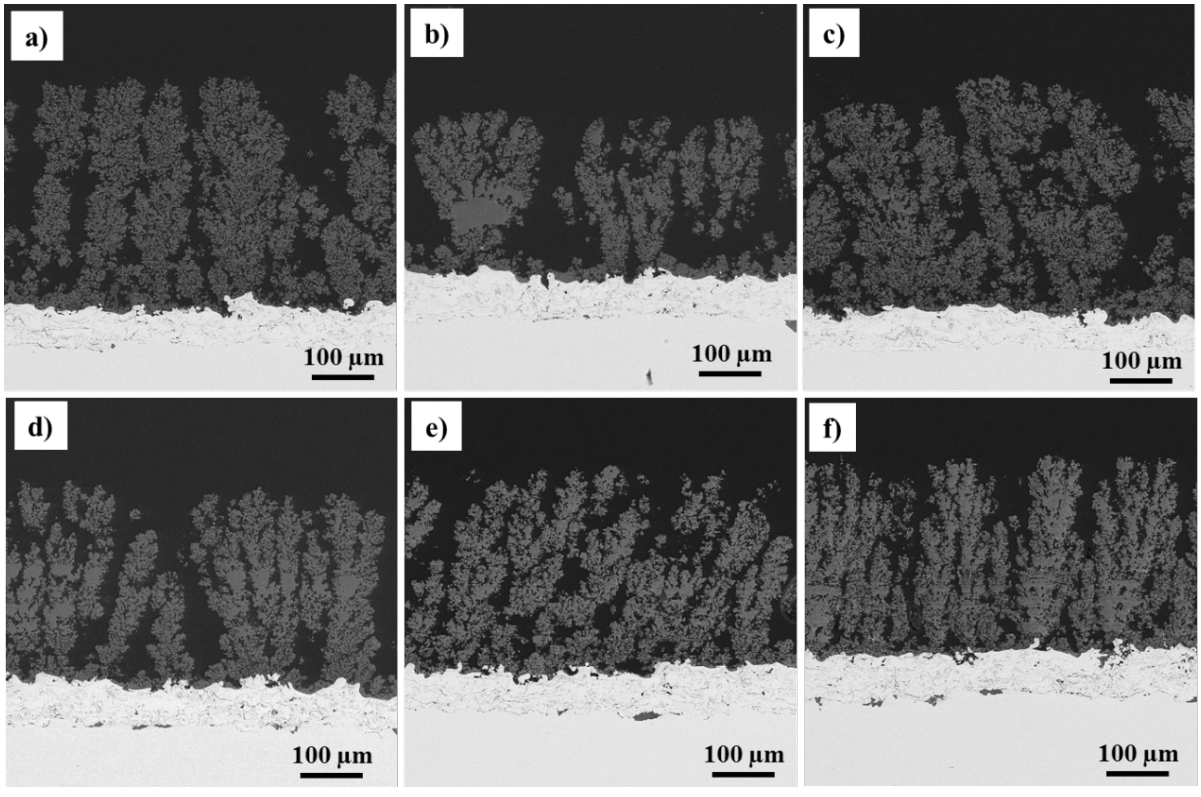

Fig. 12. Cross-section SEM images: AT3_i (a), AT3_di (b), AT13_i (c), AT13_di (d), AT40_i (e), AT40_di (f)

introduced into the hottest part of the plasma jet. This also means that not all of the powder particles will undergo a complete thermal treatment by the plasma, especially those travelling in the jet peripheries [34]. The shadowgraphy observations, presented in Figure 9, confirm this issue. Although the suspension injection pressure was set so that the mean particle trajectory was along the plasma jet axis, it is visible that some of the feedstock encountered the plasma periphery areas. It should also be noted that similar topography was observed in the alumina SPS coatings presented in the previous work [18]. Moreover, inhomogeneous melting of agglomerated powder particles has been noted also by other researchers [35]. This clearly shows that, on the one hand, a significant advantage of the proposed spraying is the possibility of tailoring any chemical composition but, on the other, the complexity of the process itself is increased, and obtaining a coating with the intended dense structure is also more difficult [36] and will demand further optimization.

Among all coatings, the AT40_di sample contained the most homogeneously distributed and melted splats. This may result from the fact that the AT40 suspension contained a higher content of TiO_2 powder, which was characterized by (i) smaller melting temperature and (ii) slightly greater particles size in comparison with Al_2O_3. Lighter and smaller particles build up the coatings with a columnar structure more easily mainly because they follow the gas swirls parallel to the bond coat/substrate and stick to the surface asperities [37].

The microstructural observations of the cross-sections confirmed the top view observations. It was revealed that all coatings, regardless of their chemical composition and type of feedstock injection, had a similar columnar-like microstructure (see Figure 12). Additionally, a significant content of intercolumnar gaps were observed in each coating. The width of the intercolumnar spacing was the smallest for the AT40 coatings (Figure 12e and 12f). Additionally, it was observed that the increased content of TiO_2 provided a higher density of columns and their uniformity. This could be combined with a low viscosity of the AT40 suspension (see section 3.1), which probably had a beneficial impact on the fragmentation of the suspension during transfer via plasma.

Spraying with the intermixed suspension as well as with the double injection showed that the range of the proposed parameters had a limited influence on the coating microstructure. An important issue seems to be the type of the used solvent. Water was preferred due to the safety of storage and environmental purposes. Nevertheless, it requires almost three times more energy for vaporization than the ethanol solvent [38]. In most cases, it is claimed that water-based suspensions provide coatings characterized by a high density and homogeneous microstructure [39], while ethanol-based ones promote the formation of columnar and porous structures [40]. However, in work [33], the authors showed that the resulting microstructure is related not only to the solvent but that the atomization of the suspension also matters. As already discussed in Figure 10, the fragmentation of the feedstock was undisturbed during the whole spray process. Therefore, it may be suspected that the obtained columnar microstructures were rather a consequence of the fine powder size but neither of the water-based solvent nor the disturbances in the suspension fragmentation.

It should be emphasized here that an extensive study on the phase composition of the alumina-titania coatings has been carried out already. Particular attention has been directed toward the stabilization of α–Al_2O_3 [18], which is a more desirable phase when compared to the metastable γ–Al_2O_3 and δ–Al_2O_3 phases [41]. However, the SPS alumina coatings generally tend to possess only a limited content of the alpha phase, because of the preferred formation of the gamma and delta phases during rapid solidification, as discussed by [42] and [43]. Indeed, in the investigated coatings, according to the XRD patterns shown in Figure 13, both the stable α–Al_2O_3 and the metastable γ–Al_2O_3 and δ–Al_2O_3 phases were observed. Unfortunately, the presence of α–Al_2O_3 in the studied coatings is mainly attributed to the presence of nonmelted powder particles, which were observed in the topography of the surfaces of the coatings. However, the content of this phase can be also in-

Table 4. Comparison of the double injection and intermixed spraying

Property	Double injection	Intermixed suspension
feedstock stability	+ easier prevention of agglomeration and sedimentation of two feedstocks separately	– stability of a mixture (suspension/suspension; suspension/powder; suspension/solution precursor) may not be easily guaranteed
waste	+ minimized material loss – the suspension after spraying can be further stored and easily used for the next spraying	– waste remains, initial suspensions cannot be separated and used again
spraying comprehensiveness	+ it opens up the possibility for a precise control of the particle thermal history, the microstructure and phase composition of coatings – the need for independent and time-consuming optimization of two feeding/injection lines – the spraying distance, angle, etc. have to be adjusted separately	+ easier optimization of spraying parameters for the injection of a single liquid
tailoring of chemical composition	– difficult selection of suspension/ solvent/ powder/ dispersing agents concentrations (especially when strong dilution is needed)	+ easy tailoring of the feedstock chemical composition
sprayability	– spraying is difficult in the case of low constituent content – there is a need to intensively dilute the suspensions; consequently, lots of energy is consumed for solvent evaporation, leading to a low process efficiency; + feasibility of the process	+ the ratio of the feedstock composition may be easily adjusted, so the disadvantages of the double injection are easily omitted

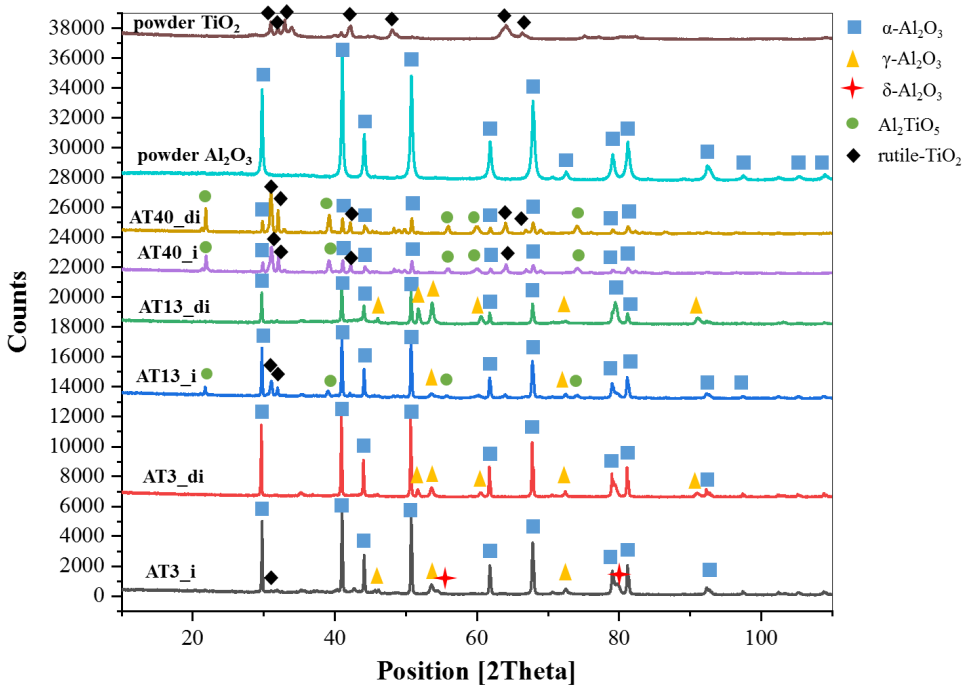

Fig. 13. Phase composition of feedstock powders and deposited coatings

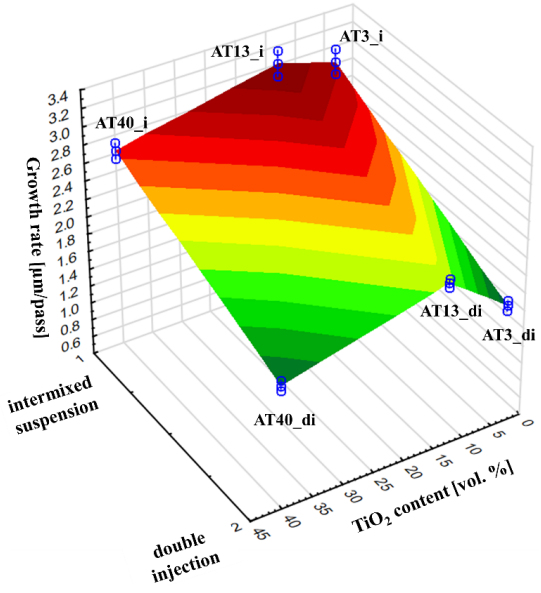

Fig. 14. Correlation between the TiO_2 content, injection manner, and the growth rate of the coatings

creased by the relatively high temperature of the substrate in the spray process (the substrate was preheated prior to spraying) [44], as well as the use of a high enthalpy plasma torch [4].

Tialite Al_2TiO_5 and rutile-TiO_2 were identified for the AT13 and AT40 coatings. As suspected, tialite was present especially in the AT40 (both AT40_i and AT40_di) coatings – for 40 wt.% TiO_2 content, this is the major phase in the Al_2O_3-TiO_2 phase diagram. Additionally, based on work [45], it is suggested that some of the initial rutile-TiO_2 in the feedstock titania powder reacted with alumina during spraying and formed the tialite phase. This could be promoted especially for the intermixed suspensions (AT13_i and AT40_i), due to the already discussed increased rate of the contact area, leading to congruent melting and mutual phase transformation [4].

The investigations showed that the differences observed in the studied alumina-titania coatings were influenced not only by different initial material properties but also by the way of feedstock introduction into the plasma jet. The summary on using the double injection or intermixed concept is provided in Table 4.

Another important advantage of the intermixed suspension spraying is the reduction of the process time and increasing the coating growth rate (Figure 14).

It should be emphasized that both the double injection and the intermixed spraying provide the possibility to formulate almost any content ratio of the used feedstocks. The tailored chemical compositions of the coatings (not limited to Al_2O_3-TiO_2 system) are of strategic importance to many industries. Consequently, it seems that the effect of the suspension characteristics on the coating properties is worth being investigated further. In the near future, it could bring measurable economic benefits, such as the extended lifetime of the components, which are key factors in the development of many new applications, like ion cells [46], solid oxide fuel cells [47], wear-resistant coatings [34], and many others. Nevertheless, due to the complexity of the process, obtaining an intended coating is a demanding task – as the obtained columnar microstructures were originally expected to be dense coatings.

4. Conclusions

The paper presents a preliminary study on hybrid SPS spraying of alumina-titania coatings: Al_2O_3 + 3 wt.% TiO_2. Al_2O_3 + 13 wt.% TiO_2. Al_2O_3 + 40 wt.% TiO_2. During the investigations, two spraying concepts, addressing multi-material feedstocks and the multi-injection approach, were considered. The studies demonstrated the promising potential of suspension plasma spraying with the intermixed suspension and double injection. The following conclusions may be drawn based on this work:

- The injection of two feedstocks via one feeding line provided a higher growth rate. As a result, the net spraying time was significantly shortened for each intermixed suspension (9.3 min) when compared to the double injection (AT3: 32.7 min, AT13: 28 min, AT40: 23.3 min).
- For the purpose of multi-injection spraying, it is especially important to use suitable di-

agnostic tools (such as shadowgraphy) for the proper setting of the feedstock injection.

- Control of the phase composition of coatings is challenging due to the rapid solidification of the sprayed feedstock and complex phase transformations but it seems possible.
- An outstanding advantage of the proposed spraying method is the possibility to deposit any selected chemical composition as unlike for the powder-based spraying methods, liquid feedstock with arbitrary composition may be prepared on-site.-.

Acknowledgements

The authors gratefully acknowledge Adam Sajbura (Wrocław University of Science and Technology, Poland) for the help during spraying. Financial support provided by National Science Centre through grant no. **2020/37/N/ST8/02825 (Development of finely grained Al_2O_3-TiO_2 coatings by hybrid suspension plasma spraying)** is gratefully acknowledged. Financial support of deposition experiments through project **19-10246S (Deposition mechanism and properties of multiphase plasma sprayed coatings prepared with liquid feedstocks)** funded by Czech Science Foundation is also gratefully acknowledged.

References

[1] Potthoff A, Kratzsch R, Barbosa M, Kulissa N, Kunze O, Toma F-L. Development and application of binary suspensions in the ternary system Cr_2O_3/TiO_2/Al_2O_3 for S-HVOF spraying. J Therm Spray Tech. 2018 Apr 1;27(4):710–7.

[2] Michalak M, Łatka L, Sokołowski P, Toma F-L, Myalska H, Denoirjean A, et al. Microstructural, mechanical and tribological properties of finely grained Al_2O_3 coatings obtained by SPS and S-HVOF methods. Surface and Coatings Technology. 2020 Dec 25;404:126463.

[3] Fauchais P, Joulia A, Goutier S, Chazelas C, Vardelle M, Vardelle A, et al. Suspension and solution plasma spraying. J Phys D: Appl Phys. 2013;46(22):224015.

[4] Tesar T, Musalek R, Lukac F, Medricky J, Cizek J, Rimal V, et al. Increasing α-phase content of alumina-chromia coatings deposited by suspension plasma spraying using hybrid and intermixed concepts. Surface and Coatings Technology. 2019 Aug 15;371:298–311.

[5] Steeper TJ, Varacalle DJ, Wilson GC, Riggs WL, Rotolico AJ, Nerz J. A design of experiment study of plasma-sprayed alumina-titania coatings. JTST. 1993 Sep 1;2(3):251–6.

[6] Alebrahim E, Tarasi F, Rahaman MdS, Dolatabadi A, Moreau C. Fabrication of titanium dioxide filtration membrane using suspension plasma spray process. Surface and Coatings Technology. 2019 Nov 25;378:124927.

[7] Musalek R, Medricky J, Tesar T, Kotlan J, Pala Z, Lukac F, et al. Suspensions plasma spraying of ceramics with hybrid water-stabilized plasma technology. J Therm Spray Tech. 2017 Jan 1;26(1):37–46.

[8] Łatka L, Michalak M, Szala M, Walczak M, Sokołowski P, Ambroziak A. Influence of 13 wt% TiO_2 content in alumina-titania powders on microstructure, sliding wear and cavitation erosion resistance of APS sprayed coatings. Surface and Coatings Technology. 2021 Mar 25;410:126979.

[9] Klyatskina E, Espinosa-Fernández L, Darut G, Segovia F, Salvador MD, Montavon G, et al. Sliding wear behavior of Al_2O_3–TiO_2 coatings fabricated by the Suspension Plasma Spraying Technique. Tribol Lett. 2015 Jul 1;59(1):8.

[10] Łatka L, Szala M, Macek W, Branco R. Mechanical properties and sliding wear resistance of Suspension Plasma Sprayed YSZ coatings. Adv Sci Technol Res J. 2020 Dec 1;14(4):307–14.

[11] Mahade S, Mulone A, Björklund S, Klement U, Joshi S. Incorporation of graphene nano platelets in suspension plasma sprayed alumina coatings for improved tribological properties. Applied Surface Science. 2021 Dec 30;570:151227.

[12] Mukherjee B, Asiq Rahman OS, Islam A, Sribalaji M, Keshri AK. Plasma sprayed carbon nanotube and graphene nanoplatelets reinforced alumina hybrid composite coating with outstanding toughness. Journal of Alloys and Compounds. 2017 Dec 15;727:658–70.

[13] Rico A, Rodriguez J, Otero E, Zeng P, Rainforth WM. Wear behaviour of nanostructured alumina–titania coatings deposited by atmospheric plasma spray. Wear. 2009 Jun 15;267(5):1191–7.

[14] Vicent M, Bannier E, Moreno R, Salvador MD, Sánchez E. Atmospheric plasma spraying coatings from alumina–titania feedstock comprising bimodal particle size distributions. Journal of the European Ceramic Society. 2013 Dec 1;33(15):3313–24.

[15] Vicent M, Bannier E, Carpio P, Rayón E, Benavente R, Salvador MD, et al. Effect of the initial particle size distribution on the properties of suspension plasma sprayed Al_2O_3–TiO_2 coatings. Surface and Coatings Technology. 2015 Apr 25;268:209–15.

[16] Darut G, Klyatskina E, Valette S, Carles P, Denoirjean A, Montavon G, et al. Architecture and phases composition of suspension plasma sprayed alumina–titania submicrometer-sized coatings. Materials Letters. 2012 Jan 15;67(1):241–4.

[17] Michalak M, Sokołowski P, Szala M, Walczak M, Łatka L, Toma F-L, et al. Wear behavior analysis of Al_2O_3 coatings manufactured by APS and HVOF spraying processes using powder and suspension feedstocks. Coatings. 2021 Aug;11(8):879.

[18] Michalak M, Toma F-L, Latka L, Sokolowski P, Barbosa M, Ambroziak A. A study on the microstructural characterization and phase compositions of thermally sprayed Al_2O_3-TiO_2 coatings obtained from powders and water-

based suspensions. Materials. 2020 Jan;13(11):2638.
[19] Berger L-M, Sempf K, Sohn YJ, Vaßen R. Influence of feedstock powder modification by heat treatments on the properties of APS-sprayed Al_2O_3-40% TiO_2 coatings. J Therm Spray Tech. 2018 Apr 1;27(4):654–66.
[20] Sarikaya O, Anik S, Aslanlar S, Cem Okumus S, Celik E. Al–Si/B_4C composite coatings on Al–Si substrate by plasma spray technique. Materials & Design. 2007 Jan 1;28(9):2443–9.
[21] Li N, Li G, Wang H, Kang J, Dong T, Wang H. Influence of TiO_2 content on the mechanical and tribological properties of Cr_2O_3-based coating. Materials & Design. 2015 Dec 25;88:906–14.
[22] Ganvir A, Björklund S, Yao Y, V. S. S. Vadali S, Klement U, Joshi S. A facile approach to deposit graphenaceous composite coatings by Suspension Plasma Spraying. Coatings. 2019 Mar;9(3):171.
[23] Tian W, Wang Y, Yang Y. Three body abrasive wear characteristics of plasma sprayed conventional and nanostructured Al_2O_3-13%TiO_2 coatings. Tribology International. 2010 May 1;43(5):876–81.
[24] Winnicki M. Advanced Functional metal-ceramic and ceramic coatings deposited by low-pressure cold spraying: a review. Coatings. 2021 Sep;11(9):1044.
[25] Ortiz CH, Hernandez-Rengifo E, Guerrero A, Aperador W, Caicedo JC. Mechanical and tribological properties evolution of $[Si_3N_4/Al_2O_3]_n$ multilayer coatings. Tribol Ind. 2021 Mar 15;43(1):23–39.
[26] Björklund S, Goel S, Joshi S. Function-dependent coating architectures by hybrid powder-suspension plasma spraying: Injector design, processing and concept validation. Materials & Design. 2018 Mar 15;142:56–65.
[27] Murray JW, Leva A, Joshi S, Hussain T. Microstructure and wear behaviour of powder and suspension hybrid Al_2O_3–YSZ coatings. Ceramics International. 2018 May 1;44(7):8498–504.
[28] Kiilakoski J, Puranen J, Heinonen E, Koivuluoto H, Vuoristo P. Characterization of powder-precursor HVOF-sprayed Al_2O_3-YSZ/ZrO_2 coatings. J Therm Spray Tech. 2019 Jan 1;28(1):98–107.
[29] Sadeghi E, Markocsan N, Joshi S. Advances in corrosion-resistant thermal spray coatings for renewable energy power plants. Part I: effect of composition and microstructure. J Therm Spray Tech. 2019 Dec 1;28(8):1749–88.
[30] Darut G, Klyatskina E, Valette S, Carles P, Denoirjean A, Montavon G, et al. Architecture and phases composition of suspension plasma sprayed alumina–titania submicrometer-sized coatings. Materials Letters. 2012 Jan 15;67(1):241–4.
[31] Sánchez E, Moreno A, Vicent M, Salvador MD, Bonache V, Klyatskina E, et al. Preparation and spray drying of Al_2O_3–TiO_2 nanoparticle suspensions to obtain nanostructured coatings by APS. Surface and Coatings Technology. 2010 Nov 15;205(4):987–92.
[32] Toma F-L, Potthoff A, Berger L-M, Leyens C. Demands, potentials, and economic aspects of thermal spraying with suspensions: a critical review. J Therm Spray Tech. 2015 Oct 1;24(7):1143–52.
[33] Tesar T, Musalek R, Medricky J, Kotlan J, Lukac F, Pala Z, et al. Development of suspension plasma sprayed alumina coatings with high enthalpy plasma torch. Surface and Coatings Technology. 2017 Sep 25;325:277–88.
[34] Huan Y, Wu K, Li C, Liao H, Debliquy M, Zhang C. Micro-nano structured functional coatings deposited by liquid plasma spraying. J Adv Ceram. 2020 Oct 1;9(5):517–34.
[35] Goel S, Björklund S, Curry N, Govindarajan S, Wiklund U, Gaudiuso C, et al. Axial Plasma Spraying of mixed suspensions: a case study on processing, characteristics, and tribological behavior of Al_2O_3-YSZ coatings. Applied Sciences. 2020 Jan;10(15):5140.
[36] Chidambaram Seshadri R, Sampath S. Characteristics of conventional and cascaded arc plasma spray-deposited ceramic under standard and high-throughput conditions. J Therm Spray Tech. 2019 Apr 1;28(4):690–705.
[37] Sokołowski P, Kozerski S, Pawłowski L, Ambroziak A. The key process parameters influencing formation of columnar microstructure in suspension plasma sprayed zirconia coatings. Surface and Coatings Technology. 2014 Dec 15;260:97–106.
[38] Fazilleau J, Delbos C, Rat V, Coudert JF, Fauchais P, Pateyron B. Phenomena involved in Suspension Plasma Spraying Part 1: suspension injection and behavior. Plasma Chem Plasma Process. 2006 Aug 1;26(4):371–91.
[39] Toma F-L, Berger L-M, Stahr CC, Naumann T, Langner S. Microstructures and functional properties of suspension-sprayed Al_2O_3 and TiO_2 coatings: an overview. J Therm Spray Tech. 2010 Jan 1;19(1–2):262–74.
[40] Müller P, Killinger A, Gadow R. Comparison between High-Velocity Suspension Flame Spraying and Suspension Plasma Spraying of alumina. J Therm Spray Tech. 2012 Dec 1;21(6):1120–7.
[41] Stahr CC, Saaro S, Berger L-M, Dubsky J, Neufuss K, Herrmann M. Dependence of the stabilization of α-alumina on the spray process. Journal of Thermal Spray Technology. 2007;16(5–6):822–30.
[42] Chráska P, Dubsky J, Neufuss K, Písacka J. Alumina-base plasma-sprayed materials part I: Phase stability of alumina and alumina-chromia. J Therm Spray Tech. 1997 Sep 1;6(3):320–6.
[43] Cipri F, Marra F, Pulci G, Tirillò J, Bartuli C, Valente T. Plasma sprayed composite coatings obtained by liquid injection of secondary phases. Surface and Coatings Technology. 2009 May 25;203(15):2116–24.
[44] Jiang X-Y, Hu J, Jiang S-L, Wang X, Zhang L-B, Li Q, et al. Effect of high-enthalpy atmospheric plasma spraying parameters on the mechanical and wear resistant properties of alumina ceramic coatings. Surface and Coatings Technology. 2021 Jul 25;418:127193.
[45] Bannier E, Vicent M, Rayón E, Benavente R, Salvador MD, Sánchez E. Effect of TiO_2 addition on the mi-

crostructure and nanomechanical properties of Al_2O_3 Suspension Plasma Sprayed coatings. Applied Surface Science. 2014 Oct 15;316:141–6.

[46] Dai L, Wang T, Jin B, Liu N, Niu Y, Meng W, et al. γ-Al_2O_3 coating layer confining zinc dendrite growth for high stability aqueous rechargeable zinc-ion batteries. Surface and Coatings Technology. 2021 Dec 15;427:127813.

[47] Lee JG, Jeon OS, Ryu KH, Park MG, Min SH, Hyun SH, et al. Effects of 8 mol% yttria-stabilized zirconia with copper oxide on solid oxide fuel cell performance. Ceramics International. 2015 Jul;41(6):7982–8.

Received 2022-02-08
Accepted 2022-03-30